Neutron-Induced Radiation Damage in LYSO, BaF_2, and PWO Crystals

Chen Hu, *Member, IEEE*, Fan Yang, *Member, IEEE*, Liyuan Zhang, *Member, IEEE*, Ren-Yuan Zhu, *Senior Member, IEEE*, Jon Kapustinsky, *Senior Member, IEEE*, Michael Mocko, Ron Nelson, and Zhehui Wang, *Member, IEEE*

***Abstract*— One crucial issue for the application of scintillation crystals in future high-energy physics experiments is radiation damage in a severe radiation environment, such as the high luminosity large hadron collider. While radiation damage induced by ionization dose in inorganic scintillators is well understood, investigations are ongoing to understand radiation damage induced by hadrons, including both charged hadrons and neutrons. Aiming at understanding neutron-induced radiation damage in fast inorganic scintillators, lutetium yttrium oxyorthosilicate (LYSO)/lutetium fine silicate (LFS), BaF_2, and PWO crystals were irradiated at Los Alamos Neutron Science Center by a combination of particles, including neutrons, protons, and γ-rays. The results indicate that LYSO/LFS and BaF_2 crystal plates are radiation hard up to a 1-MeV equivalent neutrons fluence of 9×10^{15} equivalent neutron $(n_{eq})/cm^2$, but not PWO, and the neutron-induced radiation damage in LYSO crystals is a factor of ten less than protons.**

***Index Terms*— BaF_2, LYSO, neutron, PWO, radiation damage, scintillators.**

I. Introduction

PHOTONS and electrons are fundamental particles. Total absorption electromagnetic calorimeter (ECAL) made of inorganic crystal scintillators provides the best energy resolution and detection efficiency for photon and electron measurements, enhancing physics discovery potential for high-energy physics (HEP) and nuclear physics experiments. It is thus the choice of those experiments where ultimate energy resolution is required. One crucial issue, however, is the radiation damage of inorganic scintillators in the radiation environment expected by future HEP experiments at, e.g., the high luminosity large hadron collider (HL-LHC). With a 5×10^{34} cm^{-2} s^{-1} luminosity and a 3000 fb^{-1} integrated luminosity, the HL-LHC will present a radiation environment for the endcap ECAL, where up to 130-Mrad ionization dose, 3×10^{14} charged hadrons/cm^2, and 5×10^{15} 1-MeV equivalent neutron $(n_{eq})/cm^2$ are expected [1].

Ionization dose-induced radiation damage in bulk calorimeter crystals, including color center kinetics, dose rate-dependent or independent damage for crystals with or without recovery, respectively, and damage mechanism, is well understood [2]. Charged hadron-induced damage was also investigated recently [3], [4], but not neutron-induced damage.

Bright, fast, and radiation hard cerium-doped lutetium yttrium oxyorthosilicate ($Lu_{2(1-x)}Y_{2x}SiO_5$:Ce or LYSO) crystals were proposed for a LYSO/W Shashlik sampling calorimeter for the compact muon solenoid (CMS) upgrade for the HL-LHC [5]. Total-absorption LYSO crystal calorimeters were also proposed for the SuperB experiment in Europe [6] and the Mu2e experiment at Fermilab [7]. A total absorption LYSO calorimeter for the COherent Muon to Electron Transition (COMET) experiment at Japan Proton Accelerator Research Complex (J-PARC) [8], a 3-D imaging calorimeter for the high-energy cosmic radiation detection (HERD) facility experiment in space [9], and a CMS barrel timing layer (BTL) for the HL-LHC are under construction, where 4.8-Mrad ionization dose, 2.5×10^{13} charged hadrons/cm^2, and 2.9×10^{14} n_{eq}/cm^2 are expected at the largest rapidity ($\eta = 1.45$) [10]. Table I lists the radiation level as a function of rapidity expected by the CMS minimum ionization particle (MIP) timing detectors (MTDs) at the HL-LHC. The radiation level at the barrel is an order of magnitude less than the endcaps.

One of the reasons for LYSO not being chosen for some HEP experiments is its high cost due to its high melting point and high raw material cost. Alternative cost-effective fast crystals are under investigation. The Mu2e experiment at Fermilab, for example, is building an undoped CsI total absorption calorimeter [11], [12] and considers an ultrafast yttrium-doped barium fluoride (BaF_2:Y) total absorption calorimeter for its upgrade Mu2e-II [13]. By using its ultrafast scintillation component with >0.5-ns decay time, a BaF_2 calorimeter promises an ultrafast BaF_2:Y calorimeter for Mu2e-II.

In this article, we report neutron-induced radiation damage in LYSO, BaF_2, and lead tungstate (PbWO4 or PWO) crystals irradiated at the Weapons Neutron Research facility of Los Alamos Neutron Science Center (LANSCE) [14] with 1-MeV equivalent neutron fluence up to 9.2×10^{15} n_{eq}/cm^2. Optical and scintillation properties of fast crystal samples were measured at the Caltech HEP Crystal Laboratory before and after

Manuscript received February 12, 2020; revised March 23, 2020; accepted April 15, 2020. Date of publication April 21, 2020; date of current version June 19, 2020. This work was supported by the U.S. Department of Energy under Grant DE-SC0011925 and Grant DE-AC52-06NA25396.

Chen Hu, Fan Yang, Liyuan Zhang, and Ren-Yuan Zhu are with the HEP, California Institute of Technology, Pasadena, CA 91125 USA (e-mail: zhu@hep.caltech.edu).

Jon Kapustinsky, Michael Mocko, Ron Nelson, and Zhehui Wang are with the Physics Department, Los Alamos National Laboratory, Los Alamos, NM 87545 USA.

Color versions of one or more of the figures in this article are available online at http://ieeexplore.ieee.org.

Digital Object Identifier 10.1109/TNS.2020.2989116

TABLE I
INTEGRATED RADIATION DOSE AND RATE EXPECTED BY THE CMS MIP TIMING DETECTOR AT THE HL-LHC

CMS MTD	η	n_{eq} (cm^{-2})	n_{eq} Flux ($cm^{-2}s^{-1}$)	Protons (cm^{-2})	p Flux ($cm^{-2}s^{-1}$)	Dose (Mrad)	Dose rate (rad/h)
Barrel	0.00	2.5×10^{14}	2.8×10^{6}	2.2×10^{13}	2.4×10^{5}	2.7	108
Barrel	1.15	2.7×10^{14}	3.0×10^{6}	2.4×10^{13}	2.6×10^{5}	3.8	150
Barrel	1.45	2.9×10^{14}	3.2×10^{6}	2.5×10^{13}	2.8×10^{5}	4.8	192
Endcap	1.60	2.3×10^{14}	2.5×10^{6}	2.0×10^{13}	2.2×10^{5}	2.9	114
Endcap	2.00	4.5×10^{14}	5.0×10^{6}	3.9×10^{13}	4.4×10^{5}	7.5	300
Endcap	2.50	1.1×10^{15}	1.3×10^{7}	9.9×10^{13}	1.1×10^{6}	26	1020
Endcap	3.00	2.4×10^{15}	2.7×10^{7}	2.1×10^{14}	2.3×10^{6}	68	2700

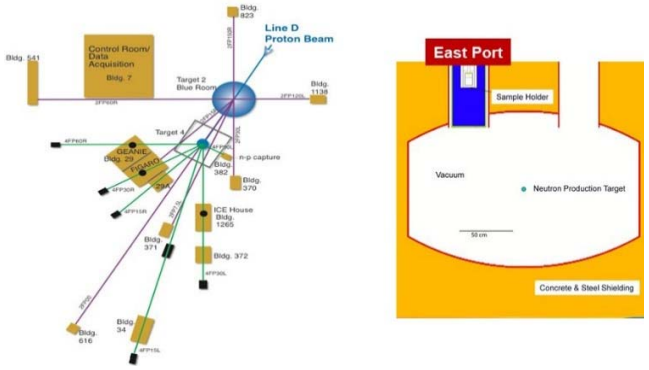

Fig. 1. Two schematics showing (left) 800-MeV proton beam line layout of LANSCE and (right) Target 4 area with the neutron production target at the center and the sample location at the East Port.

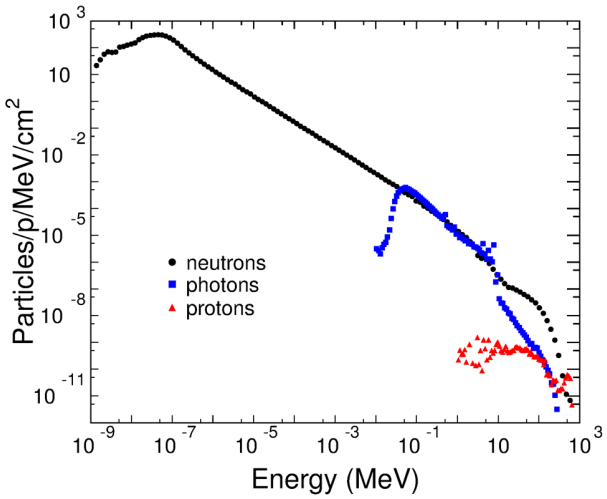

Fig. 2. Particle production rate at the East Port of LANSCE per 800-MeV proton hitting the target is shown as a function of the particle energy.

Fig. 3. Two photographs showing (left) three LFS plate bars and (right) sample holder hosting samples for experiment 6991.

irradiations. The result of this investigation is important for an optical-based radiation hard calorimeter [5] as well as the CMS BTL detector at the HL-LHC.

II. EXPERIMENTAL DETAILS AND SAMPLES

Three neutron irradiation experiments 6991, 7332, and 7638 were carried out in 2015, 2016, and 2017, respectively, at the East Port of LANSCE. Fig. 1 shows the 800-MeV proton beam line layout of LANSCE (left) and the East Port at the Target-4 site (right) [14]. Crystal samples were located in the East Port about 1.2 m away from the neutron production target.

Fig. 2 shows the particle production rate per 800-MeV proton hitting the neutron production target as a function of the particle energy for neutrons, protons, and photons from 10^{-9} to 10^{3} MeV, which were tallied on the sample volume (averaging) at the East Port. These rates are calculated by using a Monte Carlo N-Particle eXtended (MCNPX) transport package [15] developed by LANSCE. Samples were irradiated by a combination of neutrons, protons, and photons. 1-MeV equivalent neutron fluence is calculated by the neutron rate, as shown in Fig. 2, according to the nonionizing energy loss (NIEL) cross section as a function of the neutron energy [16].

In experiment 6991, a total of 18 lutetium fine silicate (LFS, which is identical to LYSO in performance) plates of 14 mm × 14 mm × 1.5 mm were attached to three plastic bars as shown in Fig. 3 (left). These LFS/LYSO plates were produced at Beijing Opto-Electronics Technology Company, Ltd. (OET) in a joint venture with Zecotek Photonics Inc. Fig. 3 (right) shows the sample holder. The LFS/LYSO plates were divided into three groups of six each in the holder, which was downloaded into the East Port before irradiation, and were retrieved one group at a time after 13.4, 54.5, and 118 days.

In experiment 7332, a total of 36 samples produced by Shanghai Institute of Ceramics (SIC), including 12 each of LYSO plates of 10 mm × 10 mm × 5 mm, and BaF_2 and PWO plates of 15 mm × 15 mm × 5 mm, were divided

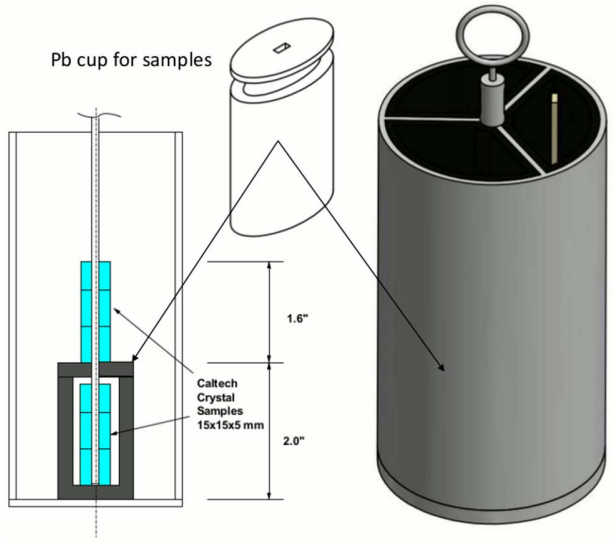

Fig. 4. (Right) 3-D sketch of the sample holder with three chambers. (Left) Cross section showing samples in one chamber, where half samples at the bottom were shielded by (top) 5-mm Pb cup and another half were not for experiment 7332.

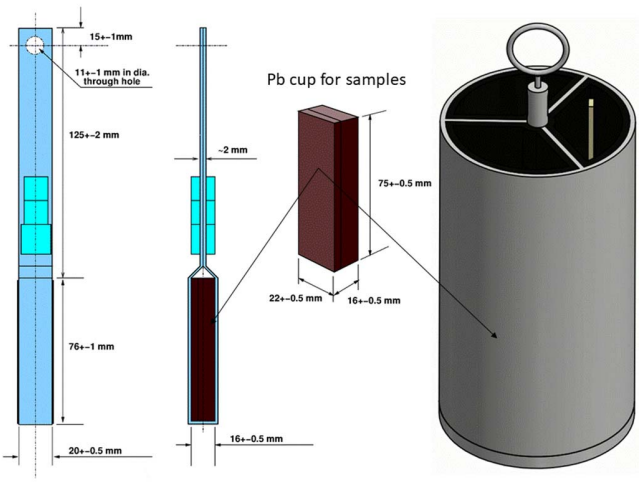

Fig. 5. (Right) 3-D sketch of the sample holder with three chambers. (Left) Cross section showing samples in one chamber, where half samples at the bottom are shielded by (middle) 5-mm Pb and another half are not for experiment 7638.

into three groups of four samples of each crystal type in each group. Half of the samples were placed inside a 5-mm-thick Pb cup as shown in Fig. 4 (top). Fig. 4 also shows a 3-D sketch of a plastic sample holder with three chambers (right) and its cross section (left). The three groups were retrieved one group at a time after 21.2, 46.3, and 120 days. This 5-mm lead shielding reduced the ionization dose by about 30% integrated over the γ-ray spectrum, but had no effect on the neutron fluence.

In experiment 7638, six LYSO plates of 10 mm × 10 mm × 1.5 mm produced by SIC, six LYSO plates of 10 mm × 10 mm × 3 mm produced by Sichuan Tianle Photonics Company, Ltd. (Tianle), and three LuAG plates of Φ14 × 1 mm^3 produced by SIC were divided into three groups of five each. They were retrieved one group at a time after 21, 48, and 102 days. In addition, eight each of BaF_2:Y and BaF_2 plates of 10 mm × 10 mm × 2 mm produced by SIC and Beijing Glass Research Institute were also in groups 1 and 3, and irradiated for 21 and 102 days, respectively. Similar to experiment 7332, half of the samples were placed inside 5-mm-thick Pb cups shown in Fig. 5 (middle). Fig. 5 also shows a 3-D sketch of a plastic sample holder with three chambers (right) and its cross section (left).

Tables II–IV list the integrated particle fluences and dose for three groups of samples without lead shielding in experiments 6991, 7332, and 7638, respectively. Fluence of fast neutrons (>1 MeV), very fast neutrons (>20 MeV), 1-MeV equivalent neutrons (in bold), protons (>1 MeV), and photon doses are also shown in these tables. The error of the neutron fluence is about 10%. The corresponding 1-MeV equivalent neutron fluences are up to 9.2, 8.3, and 6.7 × 10^{15} n_{eq}/cm^2 for experiments 6991, 7332, and 7638, respectively. We note that the proton fluence is about 800 times lower than the 1-MeV equivalent neutron fluence.

All samples were wrapped with aluminum foil to avoid optical bleach and were stored at room temperature.

TABLE II

INTEGRATED PARTICLE FLUENCES AND DOSE FOR THE CRYSTAL SAMPLES IRRADIATED IN EXPERIMENT 6991

Particles	Group-1 Fluence (cm^{-2})	Group-2 Fluence (cm^{-2})	Group-3 Fluence (cm^{-2})
Thermal and Epithermal Neutrons (0 < En < 1 eV)	1.0×10^{15}	4.6×10^{15}	9.8×10^{15}
Slow and Intermediate Neutrons (1 eV < En <1 MeV)	3.7×10^{15}	1.7×10^{16}	3.6×10^{16}
Fast Neutron Fluence (En > 1 MeV)	4.1×10^{14}	1.9×10^{15}	3.9×10^{15}
Very Fast Neutron Fluence (En > 20 MeV)	7.7×10^{13}	3.6×10^{14}	7.5×10^{14}
1 MeV Equivalent Neutron Fluence	$\mathbf{9.4\times10^{14}}$	$\mathbf{4.3\times10^{15}}$	$\mathbf{9.2\times10^{15}}$
Proton Fluence (Ep > 1 MeV)	1.2×10^{12}	5.4×10^{12}	1.2×10^{13}
Photon Dose (rad)	5.9×10^{5}	2.7×10^{6}	5.7×10^{6}

TABLE III

INTEGRATED PARTICLE FLUENCES AND DOSE FOR THE CRYSTAL SAMPLES IRRADIATED IN EXPERIMENT 7332

Particles	Group-1 Fluence (cm^{-2})	Group-2 Fluence (cm^{-2})	Group-3 Fluence (cm^{-2})
Thermal and Epithermal Neutrons (0 < En < 1 eV)	1.8×10^{15}	4.0×10^{15}	8.9×10^{15}
Slow and Intermediate Neutrons (1 eV < En <1 MeV)	6.7×10^{15}	1.4×10^{16}	3.2×10^{16}
Fast Neutron Fluence (En > 1 MeV)	7.4×10^{14}	1.6×10^{15}	3.6×10^{15}
Very Fast Neutron Fluence (En > 20 MeV)	1.4×10^{14}	3.0×10^{14}	6.8×10^{14}
1 MeV Equivalent Neutron Fluence	$\mathbf{1.7\times10^{15}}$	$\mathbf{3.7\times10^{15}}$	$\mathbf{8.3\times10^{15}}$
Proton Fluence (Ep > 1 MeV)	2.2×10^{12}	4.7×10^{12}	1.0×10^{13}
Photon Dose (rad)	1.1×10^{6}	2.3×10^{6}	5.2×10^{6}

Their optical and scintillation performance was measured before and after irradiation. The time elapsed between the end of the irradiation and the laboratory measurement was

TABLE IV
INTEGRATED PARTICLE FLUENCES AND DOSE FOR THE CRYSTAL SAMPLES IRRADIATED IN EXPERIMENT 7638

Particles	Group-1 Fluence (cm^{-2})	Group-2 Fluence (cm^{-2})	Group-3 Fluence (cm^{-2})
Thermal and Epithermal Neutrons (0 < En < 1 eV)	1.8×10^{15}	3.6×10^{15}	7.1×10^{15}
Slow and Intermediate Neutrons (1 eV < En <1 MeV)	6.6×10^{15}	1.3×10^{16}	2.6×10^{16}
Fast Neutron Fluence (En > 1 MeV)	7.3×10^{14}	1.5×10^{15}	2.9×10^{15}
Very Fast Neutron Fluence (En > 20 MeV)	1.4×10^{14}	2.8×10^{14}	5.5×10^{14}
1 MeV Equivalent Neutron Fluence	**1.7×10^{15}**	**3.4×10^{15}**	**6.7×10^{15}**
Proton Fluence (Ep > 1 MeV)	2.1×10^{12}	4.2×10^{12}	8.4×10^{12}
Photon Dose (rad)	1.1×10^{6}	2.1×10^{6}	4.2×10^{6}

about 180, 145, and 85 days for groups 1, 2, and 3, respectively. Our previous investigation shows that no recovery was found in BaF_2 [2] and LYSO [18] at room temperature after irradiation. Emission spectrum of the samples was measured by using an Edinburgh Instruments FLS920 spectrometer. The transmittance spectrum was measured by using a PerkinElmer Lambda 950 spectrophotometer with 0.15% precision. Emission-weighted longitudinal transmittance (EWLT) was calculated using

$$\mathrm{EWLT} = \frac{\int T(\lambda)\mathrm{Em}(\lambda)d\lambda}{\int \mathrm{Em}(\lambda)d\lambda} \tag{1}$$

where $T(\lambda)$ and $\mathrm{Em}(\lambda)$ are transmittance and emission spectra. The EWLT value provides a numerical representation of the transmittance over the entire emission spectrum.

Radiation-induced absorption coefficient (RIAC) was calculated as

$$\mathrm{RIAC} = \frac{1}{l}\ln\left(\frac{T_0}{T_1}\right) \tag{2}$$

where l is the crystal length and T_0 and T_1 are the transmittances before and after irradiation, respectively. The precision of the RIAC values is about 3.5 and 1 m^{-1} for 1.5- and 5-mm-thick samples, respectively [17].

The light output (LO) of the LYSO samples before and after irradiation was measured by a Hamamatsu R1306 photomultiplier tube (PMT) with a grease coupling for 0.662-MeV γ-rays from a ^{137}Cs source. The LO of BaF_2 thin plates before and after irradiation was measured by using a Hamamatsu R2059 PMT with a grease coupling for 0.511-MeV γ-rays from a ^{22}Na source with a coincidence trigger. The systematic uncertainty of these measurements is about 1%.

According to the results of the proton irradiation experiment carried out with 800-MeV protons in the blue room at LANSCE [17], the RIAC values induced by the maximum proton fluence of 1.2×10^{13} p/cm^2 in LYSO crystals is less than 0.1 m^{-1}, which is two orders of magnitude smaller compared to the observed damage at a level of 10 m^{-1} in these experiments.

On the other hand, the RIAC values in LYSO crystals induced by the maximum ionization dose of 5.7 Mrad is about 1 m^{-1} in average for LYSO crystals from six vendors [18], so is also an order of magnitude smaller than the 10 m^{-1} observed in these experiments. The 5-mm lead shielding applied to half of the samples in experiments 7332 and 7638 thus causes a negligible effect on the radiation damage.

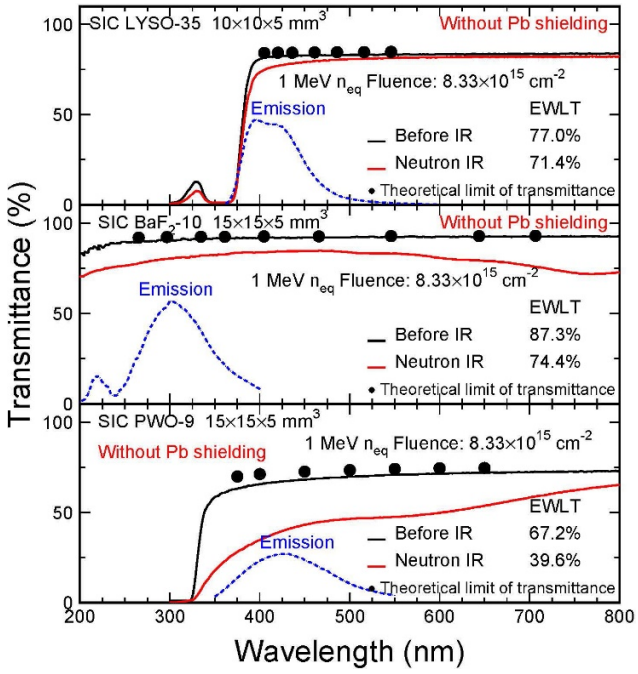

Fig. 6. Transmittance spectra measured before (black) and after (red) irradiation are shown for one sample each of (top) LYSO, (middle) BaF_2, and (bottom) PWO plates without Pb shielding in experiment 7332.

III. RESULTS AND DISCUSSION

Fig. 6 shows transmittance spectra before (black) and after (red) a 1-MeV neutron equivalent fluence of 8.3×10^{15} n_{eq}/cm^2 for one sample each of (top) the LYSO, (middle) BaF_2, and (bottom) PWO plates without Pb shielding in group 3 of experiment 7332. Also shown in the figure are the emission spectra (dashed lines), and the theoretical limit of transmittance (black dots) calculated by using crystal's refractive index assuming multiple bounces and no internal absorption [19]. Excellent optical quality was observed in these samples before irradiation. Also listed in the figure are the numerical EWLT values of 77.0%, 87.3%, and 67.2%, and 71.4%, 74.4%, and 39.6%, respectively, for LYSO, BaF_2, and PWO before and after 8.3×10^{15} n_{eq}/cm^2, indicating a much better radiation hardness of LYSO and BaF_2 than PWO.

Fig. 7 shows the LO as a function of the integration time measured before (black) and after (red) irradiation for one sample each of (top) the LYSO, (middle) BaF_2, and (bottom) PWO plates without Pb shielding in group 3 of experiment 7332. Both the LYSO and BaF_2 plates show a degradation of about 22%, which is consistent with the 25% loss observed in the LFS/LYSO plates in experiment 6991. Since the LO of the PWO samples in group 3 was too low to be measured, Fig. 7 shows instead a PWO sample in group 2 after a neutron fluence of 3.7×10^{15} n_{eq}/cm^2, which is less than half of group 3.

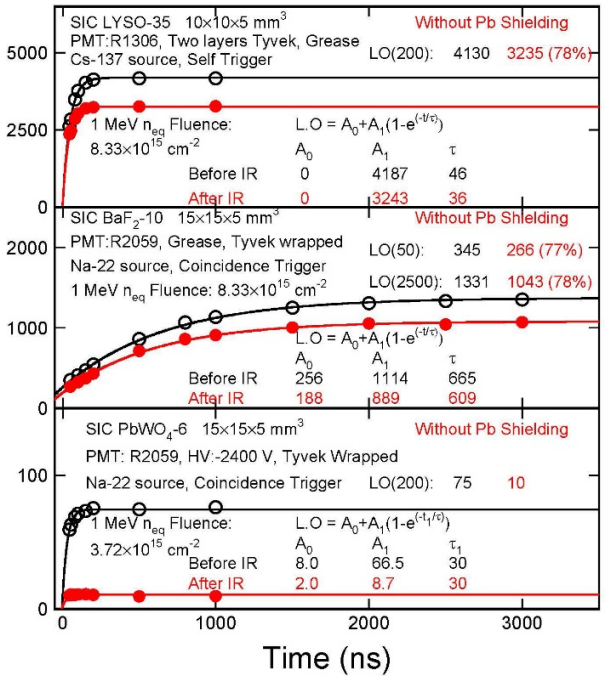

Fig. 7. LO measured before (black) and after (red) irradiation are shown as a function of the integration gate for one sample each of (top) LYSO, (middle) BaF_2, and (bottom) PWO plates without Pb shielding irradiated in experiment 7332.

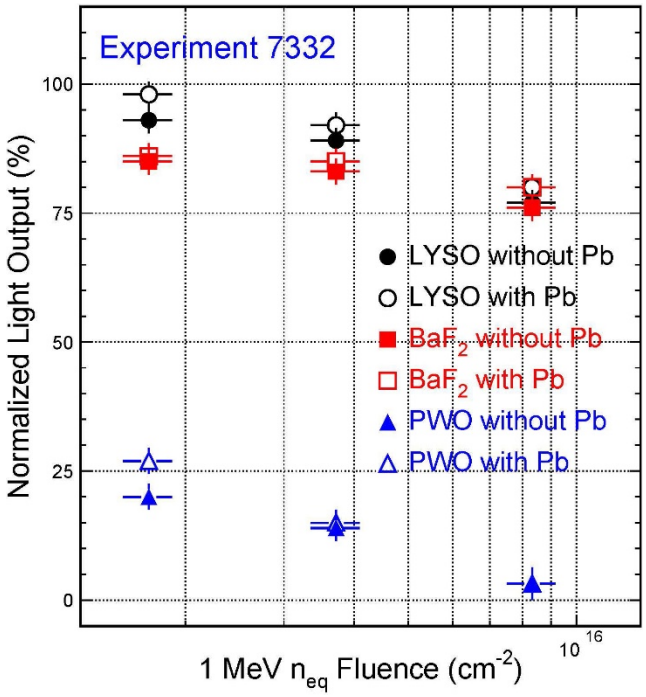

Fig. 9. Normalized LO is shown as a function of 1-MeV equivalent neutron fluence for the LYSO, BaF_2, and PWO plates irradiated in experiment 7332.

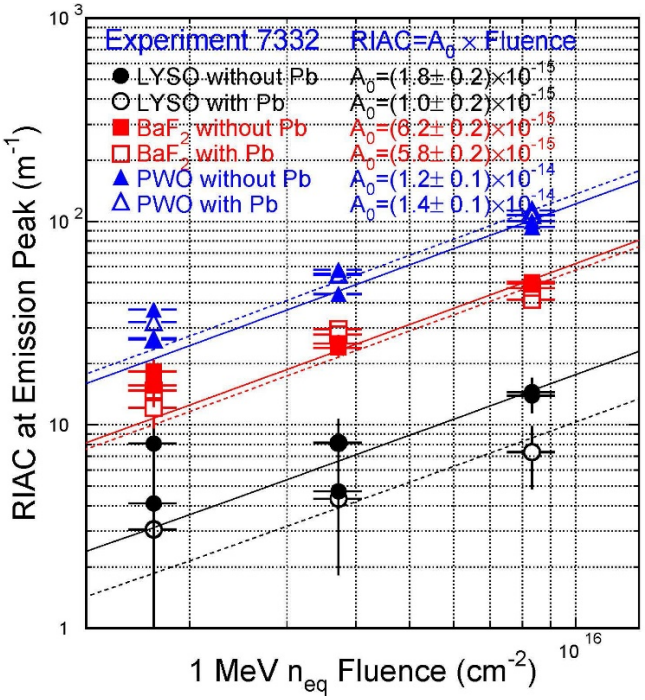

Fig. 8. RIAC values are shown as a function of 1-MeV equivalent neutron fluence for 36 LYSO, BaF_2, and PWO plates irradiated in experiment 7332.

These data show that the LYSO and BaF_2 plates are radiation hard up to 8.3×10^{15} n_{eq}/cm^2, but not the PWO plates.

Fig. 8 shows the RIAC values at the emission peak as a function of 1-MeV equivalent neutron fluence for 36 LYSO (circles), BaF_2 (squares), and PWO (triangles) plates with (open) and without (solid) 5-mm lead shielding irradiated in experiment 7332, and the corresponding linear fits. While the average RIAC values after a 1-MeV neutron fluence of 8.3×10^{15} n_{eq}/cm^2 are 14, 50, and 97 m^{-1}, respectively, for the LYSO, BaF_2, and PWO plates without 5-mm Pb shielding, they are 7.3, 44, and 111 m^{-1} with Pb shielding. These numerical values indicate that the Pb shielding might reduce the damage level in LYSO and BaF_2, but not in PWO, which can be explained by the fact that the damage induced by the ionization dose is much smaller than the damage induced by neutrons. The observed difference between with and without lead shielding thus is due to the sample-dependent variation. It is also interesting to note that BaF_2 and PWO are a factor of four and ten radiations softer than LYSO in terms of the radiation-induced absorption.

Fig. 9 shows the LO values of samples normalized to their LO values before irradiation (normalized LO) as a function of 1-MeV equivalent neutron fluence for 36 LYSO, BaF_2, and PWO plates irradiated in experiment 7332. Each LO value is an average of two samples irradiated under the same condition. The normalized LO values after a 1-MeV equivalent neutron fluence of 8.3×10^{15} n_{eq}/cm^2 are 77% and 76%, respectively, for the LYSO and BaF_2 plates without Pb shielding, and 80% and 80% with Pb shielding. It is clear that these LYSO and BaF_2 plates survive a 1-MeV equivalent neutron fluence of 8.3×10^{15} n_{eq}/cm^2 well and are much more radiation hard than PWO. It is also noticed that BaF_2 shows a larger radiation damage than LYSO after a low neutron fluence and is comparable to LYSO after a high fluence. This observation is consistent with ionization dose-induced damage in bulk calorimeter size crystals [18].

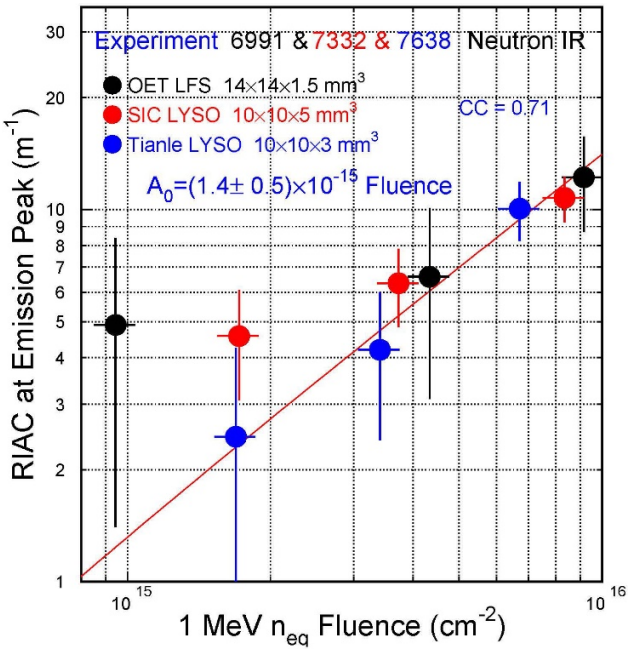

Fig. 10. RIAC values at the emission peak are shown as a function of 1-MeV equivalent neutron fluence for the LFS/LYSO plates from three vendors irradiated in three experiments.

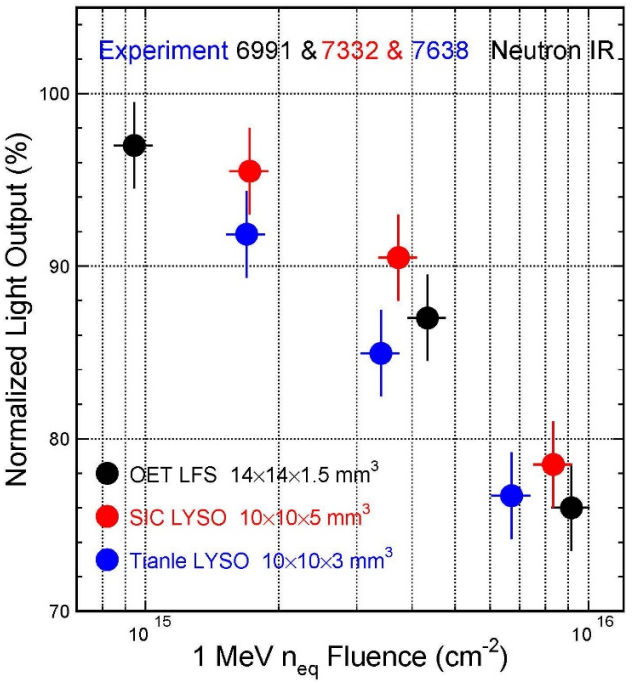

Fig. 11. Normalized LO is shown as a function of 1-MeV equivalent neutron fluence for the LYSO plates from three vendors irradiated in three experiments.

Fig. 10 shows the RIAC values at the emission peak as a function of 1-MeV equivalent neutron fluence for 18 LFS/LYSO plates from OET irradiated in experiment 6991 (black), 12 LYSO plates from SIC irradiated in experiment 7332 (red), and 6 LYSO plates from Tianle irradiated in experiment 7638 (blue), and a corresponding linear fit. All LYSO plates from different vendors show consistent neutron-induced radiation damage RIAC at 430 nm $= 1.4 \times 10^{-15}$ F_n with a correlation coefficient (CC) of 0.71, where F_n is the 1-MeV equivalent neutron fluence. This result also shows that the LYSO plates survive a 1-MeV equivalent neutron fluence up to 9×10^{15} n_{eq}/cm^2. We also notice that neutron-induced radiation damage in LYSO is a factor of ten less than damage induced by 800 MeV protons [18], [20]. This difference may be attributed to the additional ionization energy loss contribution from protons when compared to neutron-induced displacement and nuclear breakup damage.

Fig. 11 shows the normalized LO as a function of 1-MeV equivalent neutron fluence for 18 LFS/LYSO plates from OET irradiated in experiment 6991 (black), 12 LYSO plates from SIC irradiated in experiment 7332 (red), and 6 LYSO plates from Tianle irradiated in experiment 7638 (blue). Similar to Fig. 10, LYSO plates from different vendors show consistent neutron-induced radiation damage

IV. Summary

We have investigated neutron-induced radiation damage for LYSO/LFS, BaF_2, and PWO crystals at the East Port of LANSCE. LYSO crystals show the best radiation hardness among all tested crystals. Less than 25% LO loss is observed in 14 mm × 14 mm × 1.5 mm plates after a 1-MeV equivalent neutron fluence up to 9×10^{15} n_{eq}/cm^2. The RIAC at the emission peak can be factorized as RIAC at 430 nm $= 1.4 \times 10^{-15}$ F_n for commercial LYSO crystals. Such a performance meets CMS BTL radiation hardness specification: RIAC < 3 m^{-1} after a 1-MeV equivalent neutron fluence of 3×10^{14} n_{eq}/cm^2. Investigation will continue to qualify LYSO crystals from various vendors for the CMS BTL application and to understand performance of fast inorganic scintillators for future HEP experiments at the proposed future circular hadron collider (FCC-hh) facility, where 10^{18} n_{eq}/cm^2 is expected.

BaF_2 shows neutron-induced radiation damage larger than LYSO at a low neutron fluence and comparable to LYSO at a high fluence. This observation is consistent with ionization dose-induced damage in BaF_2 [18]. Investigation will continue on BaF_2:Y crystals, and to compare damage in various inorganic crystal scintillators induced by ionization dose, protons, and neutrons.

PWO crystals are found radiation soft against neutrons, which would limit its use in severe radiation environment.

While both protons and neutrons cause damage in inorganic scintillators, damage induced by protons is about an order of magnitude larger than that from neutrons, which is attributed to ionization energy loss by protons, in addition to hadron-specific damages caused by displacement and nuclear breakup.

Acknowledgment

The authors would like to thank Prof. Ke-Xun Sun of the University of Nevada, Las Vegas, for sharing the sample holders used in experiments 7332 and 7638.

References

[1] B. Bilki and The CMS Collaboration, "CMS forward calorimeters phase II upgrade," *J. Phys., Conf. Ser.*, vol. 587, Feb. 2015, Art. no. 012014.

[2] R.-Y. Zhu, "Radiation damage in scintillating crystals," *Nucl. Instrum. Methods Phys. Res. A, Accel. Spectrom. Detect. Assoc. Equip.*, vol. 413, pp. 297–311, Dec. 1998.
[3] M. Huhtinen, P. Lecomte, D. Luckey, F. Nessi-Tedaldi, and F. Pauss, "High-energy proton induced damage in PWO calorimeter crystals," *Nucl. Instrum. Methods A*, vol. 545, pp. 63–87, May 2005.
[4] R.-Y. Zhu. *A Comparison of Monitoring Data with Radiation Damage in PWO Crystals by Ionization Dose and Charged Hadron*. Accessed: Oct. 2016. [Online]. Available: http://www.hep.caltech.edu/~zhu/talks/ryz_161028_PWO_mon.pdf
[5] L. Zhang, R. Mao, F. Yang, and R.-Y. Zhu, "LSO/LYSO crystals for calorimeters in future HEP experiments," *IEEE Trans. Nucl. Sci.*, vol. 61, no. 1, pp. 483–488, Feb. 2014.
[6] G. Eigen *et al.*, "A LYSO calorimeter for the SuperB factory," *Nucl. Instrum. Methods Phys. Res. A, Accel. Spectrom. Detect. Assoc. Equip.*, vol. 718, pp. 107–109, Aug. 2013.
[7] G. Pezzullo *et al.*, "The LYSO crystal calorimeter for the Mu_2e experiment," *J. Instrum.*, vol. 9, no. 3, 2014, Art. no. C03018.
[8] K. Oishi, "An LYSO electromagnetic calorimeter for COMET at J-park," presented at the NSS, Seattle, WA, USA, Nov. 8–15, 2014, Paper O47-4.
[9] S. N. Zhang *et al.*, "The high energy cosmic-radiation detection (HERD) facility onboard China's future space station," *Proc. SPIE Int. Soc. Opt. Eng.*, vol. 9144, Jul. 2014, Art. no. 91440X.
[10] The CMS collaboration, "A MIP timing detector for the CMS phase-2 upgrade," CERN, Geneva, Switzerland, Tech. Rep. CERN-LHCC-2019-003, 2019.
[11] N. Atanov *et al.*, "Design and status of the Mu_2e crystal calorimeter," *IEEE Trans. Nucl. Sci.*, vol. 65, no. 8, pp. 2073–2080, Aug. 2018.
[12] N. Atanov *et al.*, "Quality assurance on undoped CsI crystals for the Mu_2e experiment," *IEEE Trans. Nucl. Sci.*, vol. 65, no. 2, pp. 752–757, Dec. 2018.
[13] F. Abusalma *et al.*, "Expression of interest for evolution of the Mu_2e experiment," 2018, *arXiv:1802.02599*. [Online]. Available: http://arxiv.org/abs/1802.02599
[14] *LANL and CERN for Science Community*. [Online]. Available: https://lansce.lanl.gov/facilities/wnr/flight-paths/index.php
[15] *LANL and CERN for Science Community*. [Online]. Available: https://laws.lanl.gov/vhosts/mcnp.lanl.gov/index.shtm
[16] *LANL and CERN for Science Community*. [Online]. Available: https://rd50.web.cern.ch/rd50/NIEL/default.html
[17] F. Yang, L. Zhang, R.-Y. Zhu, J. Kapustinsky, R. Nelson, and Z. Wang, "Proton-induced radiation damage in fast crystal scintillators," *IEEE Trans. Nucl. Sci.*, vol. 64, no. 1, pp. 665–672, Jan. 2017.
[18] F. Yang, L. Zhang, and R.-Y. Zhu, "Gamma-ray induced radiation damage up to 340 Mrad in various scintillation crystals," *IEEE Trans. Nucl. Sci.*, vol. 63, no. 2, pp. 612–619, Apr. 2016.
[19] D.-A. Ma and R.-Y. Zhu, "Light attenuation length of barium fluoride crystals," *Nucl. Instrum. Methods Phys. Res. A, Accel. Spectrom. Detect. Assoc. Equip.*, vol. 333, nos. 2–3, pp. 422–424, Sep. 1993.
[20] C. Hu *et al.*, "Proton induced radiation damage in fast inorganic crystals," in *Proc. IEEE Nuclear Sci. Symp. Med. Imag. Conf. (NSS/MIC)*, Manchester, U.K., 2019. [Online]. Available: http://www.hep.caltech.edu/~zhu/papers/nss19_cr_n02-5_proton%20ir.pdf